A Numerical CFD Model for Reciprocating Laminar Flow in a Channel

M. Raizner, I. Garaway and G. Grossman

Technion - Israel Institute of Technology
Haifa, Israel 32000

ABSTRACT

A CFD solution is presented for the flow and heat transfer in laminar flow in a channel under oscillating flow. An analysis of compressible flow, such as that of Helium, is preceded by that of an incompressible case; the results of the incompressible CFD model have been compared with those of an analytical solution and found to be in excellent agreement. Thus, the analytical model provides a calibration for the numerical one.

The CFD solution helps determine the effects of compressibility on the flow and heat transfer. The velocity profiles created by a reciprocating pressure difference are described. The heat transfer has been studied for a situation of a channel with insulated walls and two extreme temperatures at both ends, simulating the conditions of a pulse tube. Temperature profiles are calculated and found to depend on the flow Valensi (Va) and Reynolds (Re) numbers, on the fluid's Prandtl (Pr) number, and the Eckert (Ec) number. The convective axial heat loss was calculated and found to be non-zero despite the periodic nature of the flow.

INTRODUCTION

In recent years, many studies have been conducted to examine methods to increase the refrigeration efficiency and cooling power of pulse tube cryocoolers. The investigations, theoretical and experimental, demonstrate the complexity of design inherent to a Pulse Tube cryocooler. In light of these complexities some effort has been invested in understanding the fundamental physical phenomena taking place in the cryocooler. Understanding the oscillating compressible gas flow undergoing compression, expansion, and heat transfer is foundational to understanding the thermodynamics of the overall pulse tube Stirling cycle. Due to the complex non-linear behavior of the fluid most of the analytical studies conducted to date have simplified the actual process and treated the fluid flow as quasi-steady-state incompressible flow with constant material properties. While this assumption may be moderately valid at very low cycle frequencies and for small temperature gradients, it is far from realistic when analyzing the oscillating helium flow in a Stirling type cryocooler. The effects of the "oscillations" and temperature gradient on a real gas flow are significant and must be addressed if one wants to adequately understand the phenomena associated with this type of fluid flow. To do this accurately requires a numerical solution capable of solving the non-linear compressible flow equations. The CFD package Fluent® has recently been employed in investigating a variety of phenomena associated with cryocooler operation. Flake and Razani [1] modeled simplified but

complete pulse tube cryocoolers with some success. The results compared generally well to previously developed 1-D pulse tube models. Cha and Ghiaasiaan [2] simulated complete inertance pulse tube refrigerators, and by using the results of the study were able to adequately predict various multi-dimensional effects taking place in the cryocooler. Yarbrough and Flake [3] found that Fluent® can accurately predict the pressure drop across a wire mesh stack and proposed three different approaches to modeling regenerators.

Unlike these previously mentioned studies, this project endeavors to use Fluent to investigate basic oscillating flow phenomena, detached from overall cryocooler models. An additional uniqueness of this CFD study is that it begins by initially calibrating the model with a completely analytical solution. A similar CFD study, including calibration of the CFD model, was done by Flake and Razani [4]. They considered a circular tube and calculated the velocity profiles and the phase shift both by means of an analytical model and CFD. The CFD results corresponded well with the analytical model. We continue their work by also developing an analytical model for the temperature and heat flux profiles as well. This more complete analytical model is what is used to validate our CFD model. This CFD model, once calibrated, can be employed to investigate a variety of problems associated with oscillating compressible flow. It can be used to gain a new and credible perspective on oscillating compressible flow in a pulse tube cryocooler and its effects on the overall cycle and cryocooler device.

THEORY

Simplified Analytical Model for Incompressible Oscillating Flow

To understand the analytical model by which the CFD model was calibrated, this section will summarize briefly our previous work [5]. The general flow characteristics in an adiabatic pulse tube are represented by an oscillating flow in a two-dimensional channel with adiabatic walls. An oscillating pressure difference $\Delta P\cos\omega t$ applied between the two open ends of the channel leads to an axial oscillating flow. Solution of the continuity and momentum equations yields a one-dimensional flow with a constant pressure gradient in the x-direction, with the axial velocity independent of x and varying with y and t as follows:

$$u = \Re e\left\{ie^{i\omega t}\left(\frac{a^2\Delta P}{\mu L}\right)\frac{1}{2V^2}\left[\frac{\cosh[(1+i)V\eta]}{\cosh[(1+i)V]}-1\right]\right\}$$
(1)

here x and y are the axial and lateral coordinates, respectively; ω is the oscillating frequency; ρ,α,v and μ are the (constant) fluid density, thermal diffusivity, kinematic viscosity and dynamic viscosity; L is the channel length and a is its half-width; $\eta=y/a$ is the dimensionless lateral coordinate; and $V=(\omega a^2/2v)^{1/2}$ is a dimensionless parameter representing the ratio of oscillating inertia to viscous forces, directly related to the Valensi number (Va=$4\omega a^2/v$ =$8V^2$).

The velocity distribution (1) may now be employed in the Energy equation to determine the temperature distribution. Unlike in other analyses described in the literature, which have assumed a linear dependence of the time-average temperature on x, here the temperature distribution is not assumed, but derived. A temperature distribution consisting of a time-average term and a periodic term, in the form:

$$T = \overline{T}(x,y) + \Re e\left[\Delta T(x,y)e^{i\omega t}\right]$$
(2)

satisfies the Energy equation for incompressible flow with

$$\overline{T} = [T_H(L-x)+T_L x]\big/L$$
(3)

and

$$\Delta T = \frac{(T_H - T_L)\Delta P}{\rho \omega^2 L^2}\left[C_7 \cosh(1+i)V_1\eta + \left(\frac{Pr}{Pr-1}\right)\frac{\cosh(1+i)V\eta}{\cosh(1+i)V} \right] \tag{4}$$

here T_H and T_L are the average temperatures at the two ends of the channel, $Pr = \nu/\alpha$ is the Prandtl number, $V_1 = V\sqrt{Pr}$, and C_7 is a (complex) constant of integration, determined from the adiabatic wall boundary condition. The temperature distribution in final form depends on time, x, y and the dimensionless driving pressure ($a^4\Delta P/\rho v^2 L^2$) as follows [4]:

$$\frac{T - T_L}{T_H - T_L} = \frac{L - x}{L} + \left(\frac{a^4\Delta P}{\rho v^2 L^2}\right)A\cos(\omega t - \varphi) \tag{5}$$

where the amplitude A and phase angle φ are functions of η and of the two dimensionless Prandtl and the Valensi numbers, given explicitly in [4].

Figures 1 and 2 describe velocity and temperature profiles for a typical value of the Prandtl number (for helium) at two different values of the Valensi number. It can be seen that the profiles for the low Va resemble those for steady flow; however, those for the high Va show significant phase shifts between the velocity and temperature relative to the driving pressure. As is evident, the phase shifts vary with the lateral coordinate η. These phase shifts are a direct manifestation of the inertia associated with the increased oscillating frequency. A more detailed discussion of this behavior is given in [4].
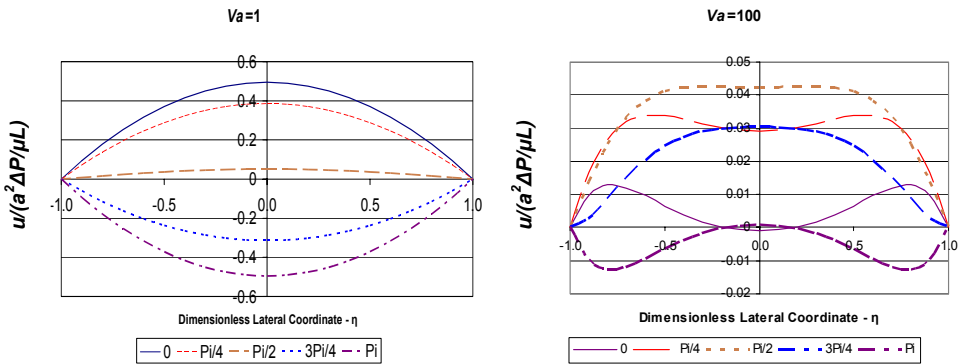

Figure 1. Velocity profiles for half a cycle for two values of the Valensi number.
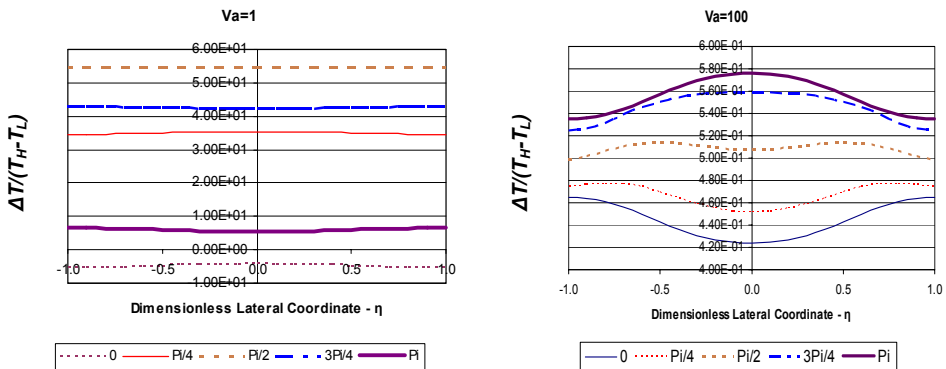

Figure 2. Temperature profiles for half a cycle at two values of the Valensi number.

Integration of the velocity over the channel width yields the total flow rate, from which an average velocity u_0 and the Reynolds number $Re=2au_0/v$ may be determined, in terms of the driving pressure ΔP. Thus, the temperature dependence on the dimensionless driving pressure $(a^4\Delta P/\rho v^2 L^2)$ in the expression (5) may be substituted for by a Reynolds number dependence.

Axial Convective Heat Transfer as a Function of Frequency

We continue, from where the previous work [4] left off, with a more complete study of the axial heat transfer in the oscillating flow, while still maintaining the assumption of incompressibility. The axial heat flux along the channel length may be written as:

$$\dot{q}'' = -k\frac{\partial T}{\partial x} + \rho u c_p (T - T_L) \tag{6}$$

where the first term on the right represents heat flux due to conduction and the second term refers to convection. Substituting the previously found solutions for the velocity and temperature profiles into (6) results in the following expression for the dimensionless axial heat flux at any cross-section x in the channel:

$$\frac{\dot{q}''L}{k(T_H - T_L)} = 1 + \left(\frac{a^2\Delta P}{\alpha\mu}\right)[U_c\cos\omega t + U_s\sin\omega t]\left|\frac{L-x}{L}\right| + \tag{7}$$

$$\left(\frac{a^4\Delta P}{\rho v^2 L^2}\right)^2\left(\frac{L}{2a}\right)^2\frac{\Pr\sqrt{\Pr}}{V^4(\Pr-1)(\sinh^2 V + \cos^2 V)}\left[\frac{U_c T_c}{2}(1+\cos 2\omega t) + \frac{U_s T_s}{2}(1-\cos 2\omega t) + \frac{(U_c T_s + U_s T_c)}{2}\sin 2\omega t\right]$$

where[1]:

$$U_c = \frac{c(V\eta)s(V) - s(V\eta)c(V)}{2V^2[c^2(V) + s^2(V)]}$$

$$U_s = \frac{c(V\eta)c(V) - s(V\eta)s(V) + c^2(V) + s^2(V)}{2V^2[c^2(V) + s^2(V)]}$$

$$T_s = \frac{[\sin V\cos V\cosh V_1\sin V_1 + \sinh V\cosh V\sinh V_1\cos V_1]s(V_1\eta)}{(\sinh^2 V_1 + \sin^2 V_1)} - \sqrt{\Pr}[s(V\eta)c(V) - c(V\eta)s(V)]$$

$$+ \frac{[\sin V\cos V\sinh V_1\cos V_1 - \sinh V\cosh V\cosh V_1\sin V_1]c(V_1\eta)}{(\sinh^2 V_1 + \sin^2 V_1)}$$

$$T_c = \frac{[\sin V\cos V\sinh V_1\cos V_1 - \sinh V\cosh V\cosh V_1\sin V_1]s(V_1\eta)}{(\sinh^2 V_1 + \sin^2 V_1)} + \sqrt{\Pr}[c(V\eta)c(V) + s(V\eta)s(V)]$$

$$- \frac{[\sin V\cos V\cosh V_1\sin V_1 + \sinh V\cosh V\sinh V_1\cos V_1]c(V_1\eta)}{(\sinh^2 V_1 + \sin^2 V_1)} - \frac{(\Pr-1)}{\sqrt{\Pr}}(\sinh^2 V + \cos^2 V)$$

In the expression (7) we can see three principal terms: The first represents the heat conduction, normalized with respect to the gradient of time-average temperature along the channel. The second represents the convective heat flux resulting from the product of local oscillating velocity by the axial time-average temperature gradient. The third term describes the heat flux resulting from the product the local oscillating velocity by the oscillating temperature. Figure 4 shows the heat flux profiles according to (7) at the center cross-section of the channel for two values of the Valensi number.

---

[1] In the following expressions, we employ the shorthand notation $c(z)=\cosh(z)\cos(z)$ and $s(z)=\sinh(z)\sin(z)$.
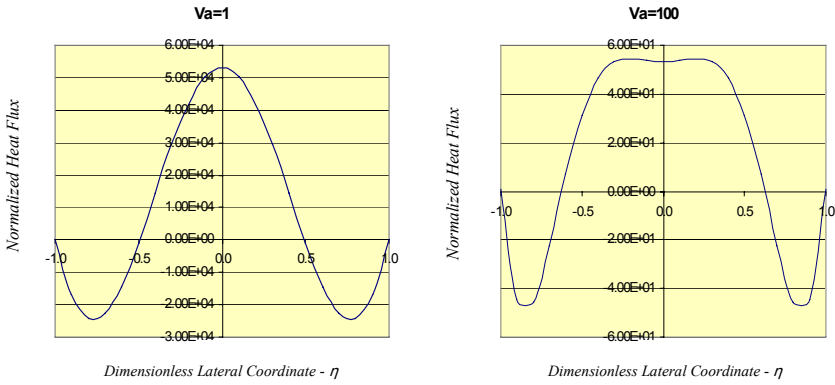
Figure 4. Convective heat flux profiles for a complete cycle at two values of the Valensi number

Integrating the expression (7) with respect to time over the period of a whole cycle yields the overall axial heat flux per cycle at any given cross-section as a result of both conduction and convection:

$$\frac{q''L}{k(T_H - T_L)} = 1 + \left(\frac{a^4 \Delta P}{\rho v^2 L^2}\right)^2 \left(\frac{L}{2a}\right)^2 \frac{\Pr\sqrt{\Pr}}{V^4 (\Pr-1)(\sinh^2 V + \cos^2 V)} \left[\frac{U_c T_c + U_s T_s}{2}\right] \qquad (8)$$

The non-linear terms in (7) stemming from the product of local velocity and temperature result in a net non-zero axial convective heat flux when averaged over the cycle time. This is in contrast with the intuitive notion that as the gas oscillates back-and-forth, so does the heat flux, in a symmetrical manner. This detrimental net heat flux from the hot to the cold end of the channel is dependent on the oscillation frequency. Figure 4 shows time-average convective heat flux profiles for two values of the Valensi number.

Integrating the expression (8) over the cross-section of the channel yields the total axial heat transferred by convection from the hot to the cold end of the channel over the cycle time. Figure 5 describes the total axial heat flux as a function of the Valensi number. The heat loss due to convection is inversely proportional to Valensi as the cycle frequency increases, perhaps contrary to intuition. This inverse relation is explained by the decrease in average velocity with an increase in the frequency of the driving pressure.
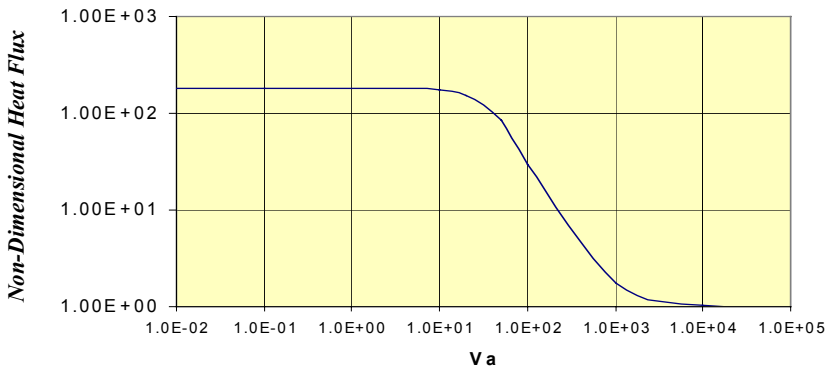

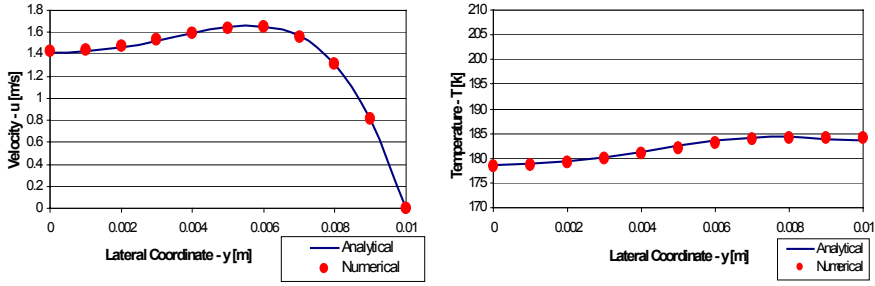**Figure 5.** Total axial heat transfer as a function of Valensi number

Figure 6. Comparison between the analytical and numerical model with respect to velocity and temperature profiles

CALIBRATION OF THE NUMERICAL CFD MODEL

The above analytical results shed light on the general behavior of the oscillating gas. The main limitation is in the assumption of incompressibility. This, along with the assumption of constant properties, limits the applicability of the model for oscillating helium flow in cryocoolers. While the analytical tool has proven very useful in describing the general behavior of the flow, a compressible model with temperature- and pressure-dependent properties must be employed to achieve quantitative accuracy in describing the actual flow. To this end, a numerical analysis was performed using the commercial CFD (Computational Fluid Dynamics) software Fluent®. Fluent® uses a finite volume discretization scheme of the momentum, continuity, and energy equations, that are sequentially solved until a pre-defined convergence tolerance is met at each time step. User inputs include the geometry and boundary conditions - specification of parameters such as pressure, temperature, velocity, mass flow rate, etc. A CFD solution may lead to erroneous results, even when convergence has been achieved. It is therefore recommended to compare them with some known results, analytical or experimental.

In the present work, to calibrate the numerical method, a Fluent® CFD model was built and solved, which matched the above-described incompressible analytical model with regard to boundary conditions and operating parameters. The resulting flow regimes, temperature, velocity, and heat flux profiles were compared with the solutions from the analytical model and were found to be essentially identical. A comparison of some representative results is given in Figure 6.

COMPRESSIBLE, TEMPERATURE DEPENDENT CFD MODEL

Once the CFD model for the incompressible case was validated, it was modified to take into account real gas behavior. The model was designed to simulate compressible, laminar, oscillating helium flow in a smooth two-dimensional channel. The channel walls are adiabatic, with time-average temperatures T_H at the hot inlet and T_L at the cold outlet. The helium properties are temperature and pressure dependent. The model and its boundary conditions are described in Figure 7. By introducing the following non-dimensional variables into the governing equations:

Non-dimensional variables:

$$\rho^* = \frac{\rho}{\rho_0};\ u^* = \frac{u}{u_0};\ x^* = \frac{x}{a};\ t^* = \omega t;\ v^* = \frac{v}{v_0};\ y^* = \frac{y}{a} \qquad T^{**} = \frac{T}{T_0}$$

$$T^* = \frac{T - T_L}{T_H - T_L};\ \alpha^* = \frac{\alpha}{\alpha_0};\ C_p^* = \frac{C_P}{C_{P_0}};\ \mu^* = \frac{\mu}{\mu_0};\ P^* = \frac{P}{\rho_0 u_0^2}$$

$$\mathrm{Re} = \frac{2au_0}{v_0};\ Va = \frac{4a^2\omega}{v_0};\ Ec = \frac{u_0^2}{c_{p_0}(T_H - T_L)}\ ;Ma = \frac{u_0}{c}\ ;\mathrm{Pr} = \frac{v}{\alpha}$$

yields the following set of dimensionless transport equations:

$$\frac{\partial \rho^*}{\partial t^*} + \frac{2\,\mathrm{Re}}{Va}\frac{\partial(\rho^* u^*)}{\partial x^*} = 0 \qquad \textbf{\textit{- Continuity}} \quad (9)$$

$$\frac{Va}{2\,\mathrm{Re}}\frac{\partial u^*}{\partial t^*} + \left[\, u^*\frac{\partial u^*}{\partial x^*} + \frac{1}{\rho^*}\frac{\partial P^*}{\partial x^*}\,\right] = \frac{2}{\mathrm{Re}}\left[\,\frac{\partial^2 u^*}{\partial x^{*2}} + \frac{\partial^2 u^*}{\partial y^{*2}}\,\right] \textbf{\textit{- Momentum}} \quad (10)$$

$$\frac{Va}{2\,\mathrm{Re}}\frac{\partial T^*}{\partial t^*} + u^*\frac{\partial T^*}{\partial x^*} = \frac{2}{\mathrm{Re}\,\mathrm{Pr}}\alpha^*\left(\frac{\partial^2 T^*}{\partial x^{*2}} + \frac{\partial^2 T^*}{\partial y^{*2}}\right) - Ec\,\frac{P^*}{\rho^* C_P^*}\frac{\partial u^*}{\partial x^*} \quad \textbf{\textit{- Energy}} \quad (11)$$

$$P^* = \frac{\rho^*}{Ma^2}\cdot\frac{T^{**}}{k} \qquad \textbf{\textit{- Ideal Gas}} \quad (12)$$
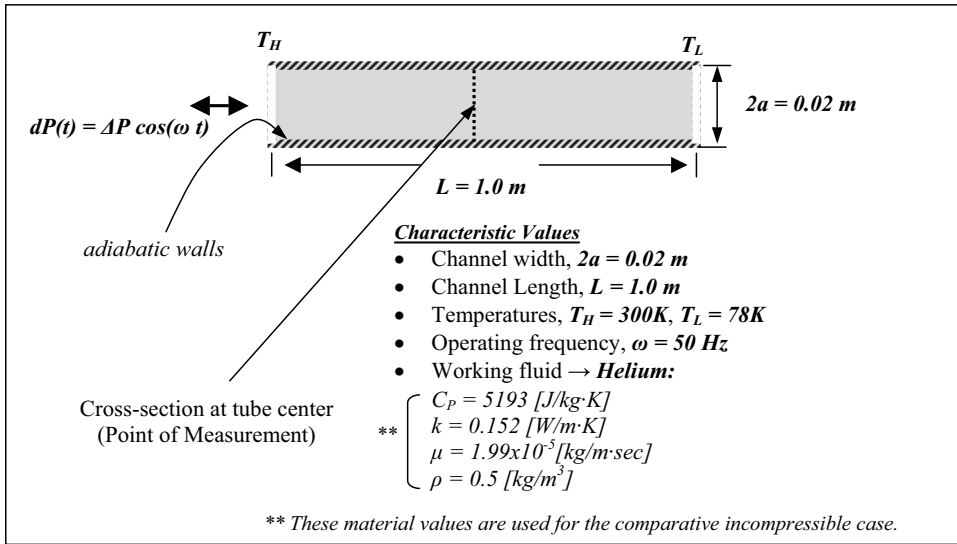

Figure 7. Characteristic values for the channel being investigated

Close examination reveals that the above model is dependent on five dimensionless parameters. The first three - Prandtl, Valensi, and Reynolds are the same as already encountered in the incompressible model. The compressible model has a fourth and fifth parameter – the Eckert Number (Ec) - representing the ratio of the kinetic energy of the flow to the fluid's enthalpy difference between the hot and cold ends. A fifth parameter - the Mach number - results from the ideal gas equation.

Verification that these are indeed the governing dimensionless parameters was conducted as follows: Two different geometry tubes with different boundary flow inputs were selected in such a way that the dimensionless parameters – Pr, Va, Re and Ec at the inlet were equal. Fluent® simulations were conducted for these two separate channel geometries being driven by different pressure differences, evaluating the complete velocity profiles along their length. The velocity profiles at the center cross-section were compared and found to be essentially identical for both tubes.

The case shown in Figure 7 was simulated for <u>compressible</u> helium flow at an oscillation frequency of 50 Hz which corresponds to a Valensi number of approximately 100. The temperature, velocity, and heat transfer profiles are shown in Figure 8, 9, and 10 in comparison to the same profiles from the incompressible model.
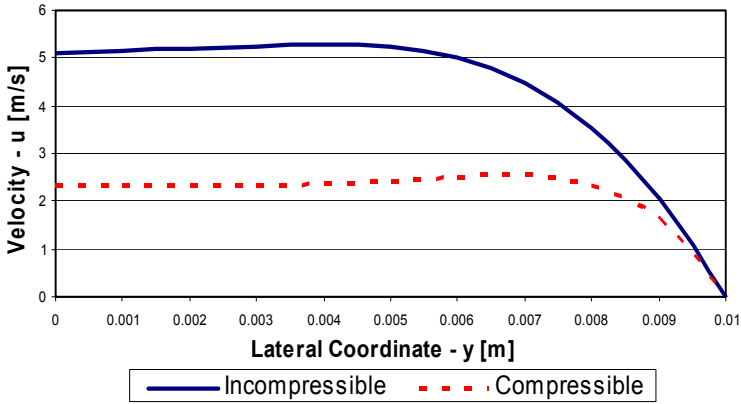
Figure 8. Comparison of velocity profiles between the compressible and
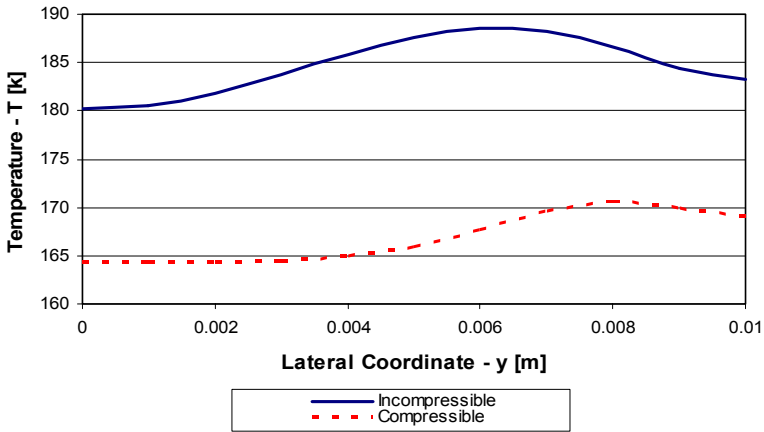incompressible case @ t = 0 (beginning of cycle)

Figure 9. Comparison of temperature profiles between the compressible and
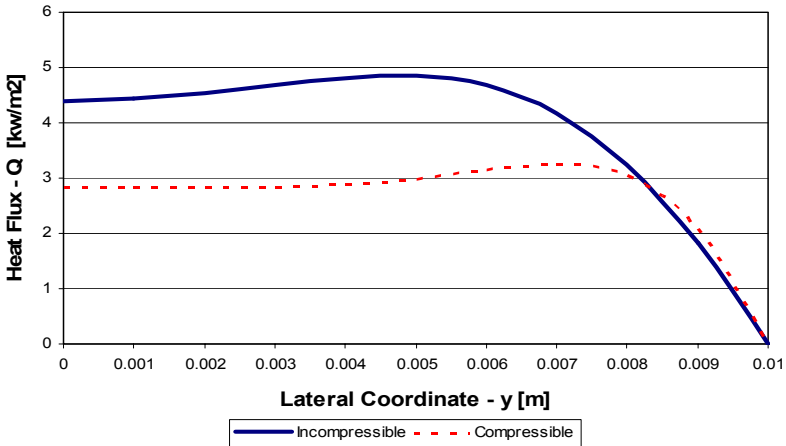incompressible case @ t = 0 (beginning of cycle)

Figure 10. Comparison of heat flux profiles between the compressible and
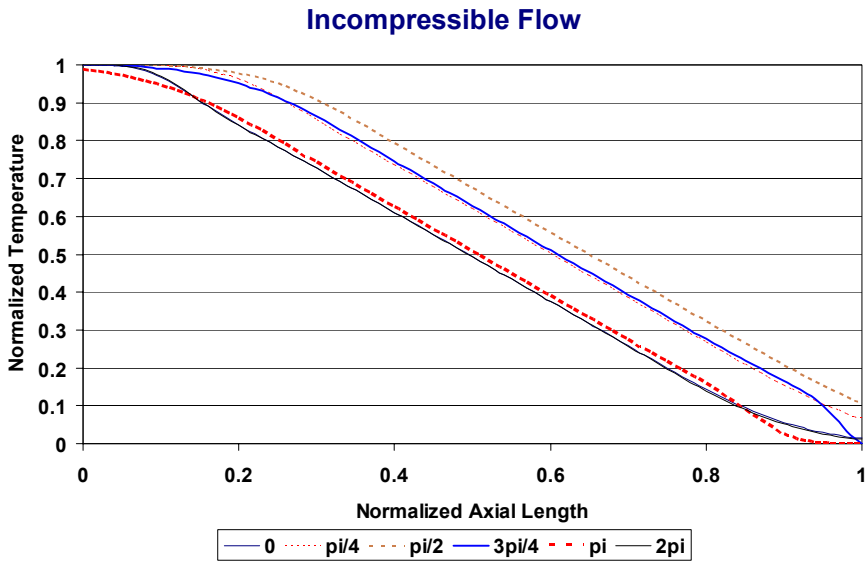incompressible case @ t = 0 (beginning of cycle)

Incompressible Flow

Figure 11. Axial temperature profiles for the incompressible case @ t = 0
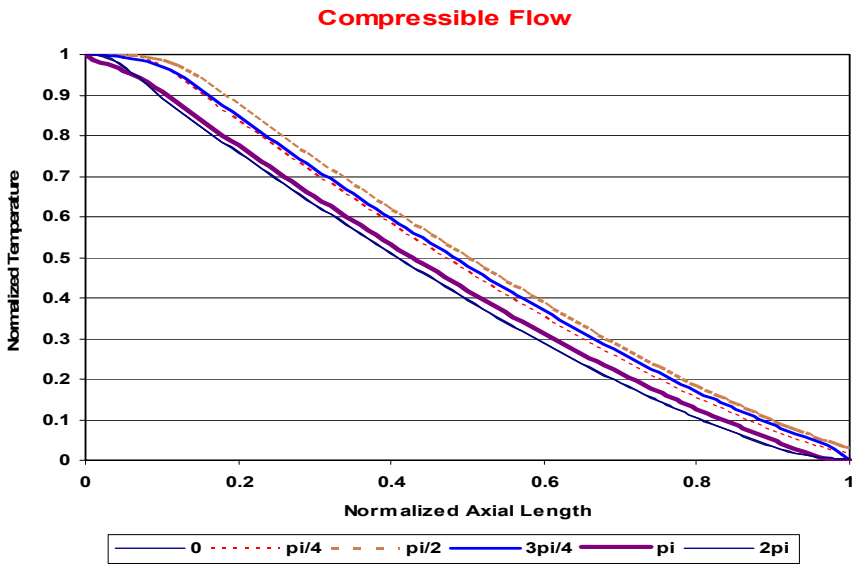(beginning of cycle)

Compressible Flow

Figure 12. Axial temperature profiles for the compressible case @ t = 0
(beginning of cycle)

The velocity profiles for the compressible flow are of smaller amplitude than those of the incompressible flow. This appears to result from the oscillating compressible flow having a higher flow resistance due to compressibility. These results are adequately discussed in our previous work [6]. The temperature profiles also have smaller amplitudes in the compressible than in the incompressible case. This is a result of their dependence on the velocity profile. The convective heat flux is also smaller in amplitude for the compressible flow, as a result of it being a product of the velocity and temperature.

Temperature profiles along the length of the channel for one half a cycle are shown in Figures 11 and 12 for the compressible and incompressible models, respectively. The non-linearity observed at the two ends of the tube is an entrance effect: The temperature in this area is heavily weighted by the fluid temperature being cycled in and out of the channel. In the incompressible case the temperature gradient is perfectly linear beyond the entrance zone. For the compressible flow the temperature gradient is no longer linear and develops a concave pattern as a result of the higher thermal capacity of the flow at the cold end.

CONCLUSION

This work has sought to establish some fundamental understanding of the oscillating gas flow present in pulse tube cryocoolers. An analytical incompressible model has provided useful information on the general behavior of this flow. It showed how the oscillating frequency shifts the phase of velocity and temperature relative to the driving pressure difference, by virtue of its inertia. The results have also shown a net convective heat flux along the tube, which can be minimized by working at higher frequencies.

A validated numerical CFD model was developed to determine the effects of compressibility and "real gas properties" on the oscillating flow. This model, initially calibrated by the analytical model, went on to calculate the velocity and temperature distributions. A dimensional analysis showed that compressible oscillating flow is dependent not only upon Va, Pr, and Re but also upon the Eckert number. This developed model can now be used as a tool to further investigate the heat and mass transfer phenomena present in various cases of pulse tubes, for example such as that found in tapered pulse tubes.

ACKNOWLEDGMENT

REFERENCES

1. Flake B., Razani A, "Modeling pulse tube cryocoolers with CFD," *Adv. in Cryogenic Engineering*, Vol. 49B, Amer. Institute of Physics, Melville, NY (2004), pp. 1493-1499.
2. Cha J.S., Ghiaasiaan S.M., et al "CFD simulation of multi-dimensional effects in an Inertance tube pulse tube refrigerator," *Cryocoolers 13*, Springer Science+Business Media, New York (2005), pp. 285-292.
3. Yarbrough S.A., Flake B.A., Razani A. "Computational fluid dynamic modeling of pressure drop through wire mesh screen regenerators" *Adv. in Cryogenic Engineering*, Vol. 49B, Amer. Institute of Physics, Melville, NY (2004), pp. 1138-1145.
4. Flake B., Razani A, "Phase shift and compressible fluid dynamics in inertance tubes" *Cryocoolers 13*, Springer Science+Business Media, New York (2005), pp. 275-285.
5. Grossman G., Nachman I, "An analytical heat transfer model for reciprocating laminar flow in a channel," *Adv. in Cryogenic Engineering*, Vol. 51, Amer. Institute of Physics, Melville, NY (2006), pp. 1580-1587.
6. Garaway I, Grossman G, "Studies in high frequency oscillating compressible flow for application in a micro regenerative cryocooler," *Adv. in Cryogenic Engineering*, Vol. 51, Amer. Institute of Physics, Melville, NY (2006), pp. 1588-1595.